Biophysical Chemistry 228 (2017) 38–46

Contents lists available at ScienceDirect

Biophysical Chemistry

journal homepage: www.elsevier.com/locate/biophyschem

Dynamical regimes of lipids in additivated liposomes with enhanced elasticity: A field-cycling NMR relaxometry approach

Carla C. Fraenza, Esteban Anoardo*

Laboratorio de Relaxometría y Técnicas Especiales (LaRTE), Grupo de Resonancia Magnética Nuclear, Facultad de Matemática, Astronomía y Física, Universidad Nacional de Córdoba and IFEG – CONICET, Ciudad Universitaria X5000HUA, Córdoba, Argentina

HIGHLIGHTS

- We discuss the first proton field-cycling NMR relaxation experiments in elasticity enhanced additivated liposomes.
- A new relaxation regime for the lipid protons is observed for the first time.
- Dramatic changes as the additive concentration is increased are revealed in the nuclear relaxation dispersion.
- The bending elastic modulus can be measured using the field-cycling NMR technique.

GRAPHICAL ABSTRACT

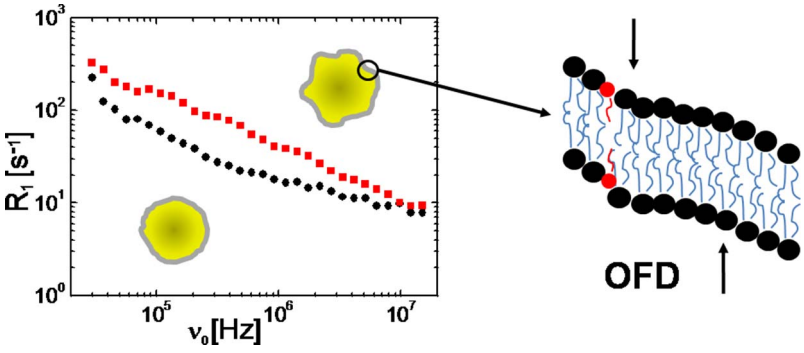

ARTICLE INFO

Keywords:
Liposomes
Membrane flexibility
Deformability
NMR relaxometry
Lipid dynamics

ABSTRACT

We study the molecular dynamics of lipids in binary large unilamellar liposomes suspended in D_2O composed of 1,2-dimyristoyl-*sn*-glycero-3-phosphocholine (DMPC) or soy phosphatidylcholine (SPC) additivated with different percentiles of sodium deoxycholate (SDC). We use the fast field-cycling proton NMR relaxometry technique over a wide timescale and at diverse temperatures. A model previously validated in different formulations is here employed for the relaxometric analysis of elastic vesicles. A new dynamical regime is observed for the first time in additivated DMPC and additivated/non-additivated SPC liposomes. This surprising feature is discussed in terms of vesicle shape fluctuations, enhanced elasticity and lipid & additive diffusion within the membrane. The continuum elastic theory is revisited for a better understanding of recent experiments and those here presented. We address the point of deformability measurements across rigid permeable barriers versus measurements of the bending elastic modulus in free-standing vesicles.

1. Introduction

The elastic properties of lipid membranes can be conveniently characterized through the bending elastic modulus κ. Reliable and non-invasive methods to characterize the elastic properties of membranes are attractive for both fundamental research and industrial applications [1,2]. Elasticity directly affects the deformability of a membrane, morphological and shape transitions, fusion, lipid-protein interactions, etc. It is also a critical property for the formulation of ultradeformable liposomes, and of interest for the design of theranostic liposomes for efficient drug delivery systems and/or different imaging contrast agents. A new method for the measurement of κ in liposome membranes based on the fast field-cycling nuclear magnetic relaxometry technique (FFC) was recently presented [3]. Main advantages of this experimental

* Corresponding author.
E-mail address: anoardo@famaf.unc.edu.ar (E. Anoardo).

http://dx.doi.org/10.1016/j.bpc.2017.06.007
Received 6 April 2017; Received in revised form 14 June 2017; Accepted 20 June 2017
Available online 27 June 2017

technique are the absolutely non-invasiveness and the possibility to test nano-devices like liposomes, polymeric vesicles, etc. of any size between just a few nanometers in diameter up to several hundreds of nanometers. This technique can also provide valuable information on the local and collective dynamics of the assembling molecules, and through them, on the mesoscopic properties of the membrane.

Liposomes with enhanced membrane elasticity (such as *menthosomes* and *transfersomes*) appear as a promising alternative for drug administration through transdermal route [4,5]. A potential advantage over conventional routes is the avoidance of first pass metabolism, which decreases drug bioavailability and generate undesirable side effects [6]. An ultradeformable liposome is a vesicle that has a highly flexible ($\kappa \leq 2k_BT$) membrane, that can be used to transport a variety of drugs through the natural pores of the skin, due to its ability to adapt its shape to the conditions of the environment [7–10].

Many experimental techniques have been used for the characterization of vesicles membrane dynamics, but most of them are only capable of monitoring a single aspect of the dynamics and/or a very limited time scale. In contrast, fast field-cycling (FFC) nuclear magnetic resonance relaxometry is sensitive to molecular and sub-molecular motions over a comparatively wide timescale, typically ranging from 10^{-3} to 10^{-9} s. The technique has been successfully applied to study the molecular dynamics in an extensive range of materials [11], and it can be used to study hydrated sub-micron sized liposomes in suspension. The experiment involves the measurement of the spin-lattice relaxation rate (R_1) as a function of the magnetic field strength (B_0), and hence ^{1}H Larmor frequency: $\nu_0 = \gamma^H B_0/2\pi$, where γ^H is the ^{1}H gyromagnetic ratio.

A physical model for interpreting the FFC ^{1}H spin-lattice relaxation rate dispersions of large unilamellar liposomes (suspended in D_2O) has already been discussed [12–14]. So far the model was validated for liposomes of different sizes, at diverse temperatures, and composed of a single component (DMPC or DOPC lipids) in the l_d phase [12,13], and DOPC-cholesterol and DMPC-cholesterol mixtures [3,14]. A striking feature is that collective order fluctuations (*OF*) of the lipid molecules are an essential dynamical process that must be taken into account in order to consistently explain the observed relaxation profiles. Since the associated *OF* relaxation mechanism directly depends on κ, its value can be obtained from the data analysis. According to this model, the relaxation rate R_1 can be described as:

$$R_1(\omega) = \frac{1}{T_1} = A_{OF}J_{OF}(\omega) + A_D J_D(\omega) + A_R J_R(\omega) + A_{FM} \quad (1)$$

Here T_1 is the spin-lattice relaxation time, $J_{OF}(\omega)$, $J_D(\omega)$ and $J_R(\omega)$ are the spectral density functions corresponding to OF (due to shape fluctuations of the vesicle), translational and rotational diffusion of lipids, respectively. A_j are the corresponding amplitudes reflecting the strength of the relevant ^{1}H-^{1}H dipolar interactions, defined as $(9/8r_j^6)\gamma^4\hbar^2(\mu_0/4\pi)^2$, where r_j is the effective inter-proton distance for the relevant dynamic process, γ the proton gyromagnetic ratio, $\hbar$ the Plank's constant divided by 2π, and μ_0 the vacuum magnetic permeability. $\omega = 2\pi\nu_0$ and A_{FM} is a frequency-independent term representing internal fast motions within the lipid molecules, which are not dispersive in the explored frequency window (note that in this approach we do not asses details of the internal individual lipid dynamics). The *OF* term, that is sensitive to κ, can be written as [15]:

$$J_{OF}(\nu)\frac{K_BT}{2\pi\kappa}\sum_{l=2}^{l_{max}}\frac{l(l+1)(2l+1)}{(l^2+l-2)(l^2+l+\sigma)}\frac{\tau_l}{[1+4\pi^2(\nu+\nu_L)^2\tau_l^2]} \quad (2)$$

where K_B is the Boltzmann constant, T is the temperature, σ is the effective lateral tension, ν_L is the offset magnetic field due to the average local field component along the quantization axis and τ_l is given by:

$$\tau_l = \frac{\eta r_v^3}{\kappa}\frac{(2l+1)(2l^2+2l-1)}{l(l+1)(l+2)(l-1)(l^2+l+\sigma)} \quad (3)$$

In the last equation η is the viscosity of the solvent, r_v the average radius of the vesicles and $l_{max} \approx \pi r_v/\delta$, where δ is the average distance between neighboring lipid molecules. Details of the other spectral densities and cross correlation couplings are not relevant for the present discussion, and can be found in reference [12].

The main goal of this work is to analyze the lipid dynamics in contrast with the elastic properties in additivated membranes with reduced stiffness ($\kappa \sim 2K_BT$). This is an important feature in view of the growing interest in the study of different processes that are directly related with membrane elasticity, especially if this can be done using non-invasive and non-destructive techniques that may be used in a size domain that is prohibitive to optical methods. Liposomes based on lipid-detergent mixtures were prepared at different concentrations. Specifically, we analyze experimental relaxation dispersions obtained at different temperatures (303–328 K) for liposomes of radius of 50 nm, composed of 1,2-dimyristoyl-*sn*-glycero-3-phosphocholine (DMPC) or soy phosphatidylcholine (SPC) with sodium deoxycholate (SDC) added to enhance the membrane flexibility, at concentrations of 3, 10 and 20 mol%.

As a part of this manuscript we include in the Supplementary Material a revision of the main physical concepts involved in membrane elasticity and instability, and we confront the concept of deformability and determinations of the bending modulus κ from extrusion experiments across solid pore membranes, with non-invasive determinations of κ in non-perturbed free-standing vesicles at thermal equilibrium. In addition, we analyze the potential effects of magnetic fields in determinations of κ using NMR techniques. See Sections S1, S2 and S3 in the Supplementary material.

2. Results and analysis

2.1. Validation of a new automatic fitting process for the analysis of the measured dispersion curves

In order to progress in the study of elastic vesicles using the field-cycling NMR technique we found important to validate a new automatic procedure for the fitting of the model to the measured data here proposed. This is an essential step in order to implement general criteria that will be used in all the cases, with the parallel advantage of a much faster analysis. However, in this procedure, a model is fitted to the data using 7 parameters, thus raising the question of how meaningful that is and how well different parameters would describe the data. It should be stressed that we only consider this option after a step by step construction of the model, based on existent dynamical processes as observed and characterized using other experimental techniques. The robustness of the model was tested for different situations and the consistence of the resulting parameters where verified. The scanned hyperspace of variables is defined by the most probable values for the parameters (still, the system under study is well known, and some information can be obtained in the literature). Please observe that some of the intervals for the parameters do not change substantially, independently of the lipid or the mixture. For a better understanding of this point, the reader is invited to follow the analysis done in references [12–14]. The validation procedure, described in detail in the supplementary material, shows that the automatic fitting allowed us to successfully reproduce previous results obtained through a manual optimization of the model curves.

In Section S4 of the Supplementary material we compare new data processed using the automatic procedure, with previous results obtained for DMPC at 310 K. In Section S5 of the Supplementary material we apply the new methodology to DMPC + cholesterol mixtures in order to test the consistency and compare with previous results and other repots obtained using different experimental techniques.

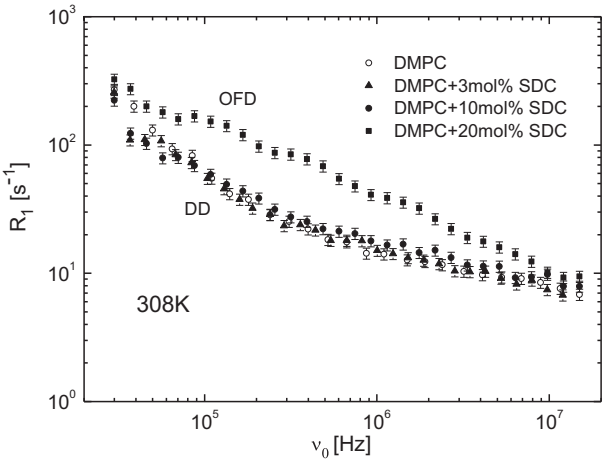

Fig. 1. Comparison of relaxation rate dispersion profiles of DMPC liposomes with 0, 3, 10 and 20 mol% SDC and average radius of 50 nm, recorded at 308 K. Observe the abrupt change in the dispersion for 20 mol%. OFD and DD stands for "Order Fluctuations Driven" and "Diffusion Driven" (see text for explanation).

2.2. Relaxation rate dispersion experiments in liposomes additivated with SDC

2.2.1. Liposomes of DMPC + SDC

Experimental relaxation rate dispersion curves $R_1(\nu_0)$ for liposomes of DMPC, with 0, 3, 10 and 20 mol% SDC, at 308 K are shown in Fig. 1, and their optimal model curves are shown in Figs. 2, 3, 4 and 5, respectively. Corresponding parameters are presented in Table 1. It is possible to observe from Fig. 1 that there is no difference, within experimental error, between curves with 0, 3 and 10 mol% SDC. In contrast, the profile of DMPC + 20 mol% SDC liposomes has a noticeable different dispersion.

It can be seen that there is a very good agreement, within experimental errors, between experimental and model curves for the three SDC percentages (see Figs. 2–5). The numerical values of all parameters are within the expected range according to literature [16–26].

The bending elastic modulus κ shows a slight tendency to decrease as the percentage of SDC increases (see Table 1). The fact that κ do not show a large variation is consistent with other studies where

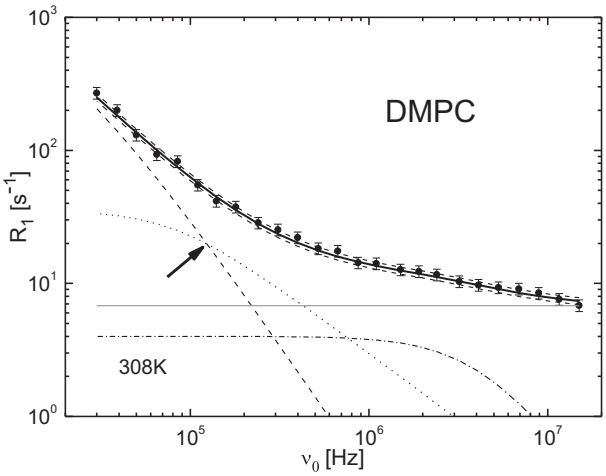

Fig. 2. Relaxation rate dispersion of DMPC liposomes with average radius of 50 nm, recorded at 308 K. Experimental points are compared with the optimal model curve (black solid line). Model curve error is shown by the two dash lines beside the black solid line. Contributions from each type of motion are included: translational diffusion (dash line), order fluctuations (dot line), molecular rotations (dash-dot line), and fast motions (solid grey line). The relevant parameters are given in Table 1. The arrow indicates the crossing point between order fluctuations and diffusion processes.

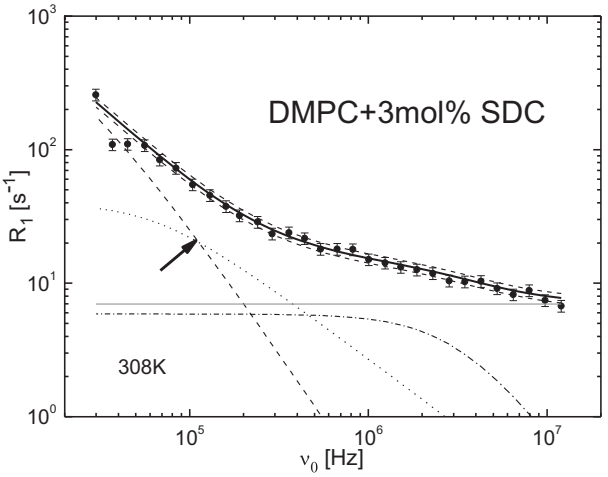

Fig. 3. Relaxation rate dispersion of DMPC + 3 mol% SDC liposomes with average radius of 50 nm, recorded at 308 K. Experimental points are compared with the optimal model curve (black solid line). Model curve error is shown by the two dash lines beside the black solid line. Contributions from each type of motion are included: translational diffusion (dash line), order fluctuations (dot line), molecular rotations (dash-dot line), and fast motions (solid grey line). The relevant parameters are given in Table 1. The arrow indicates the crossing point between order fluctuations and diffusion processes.

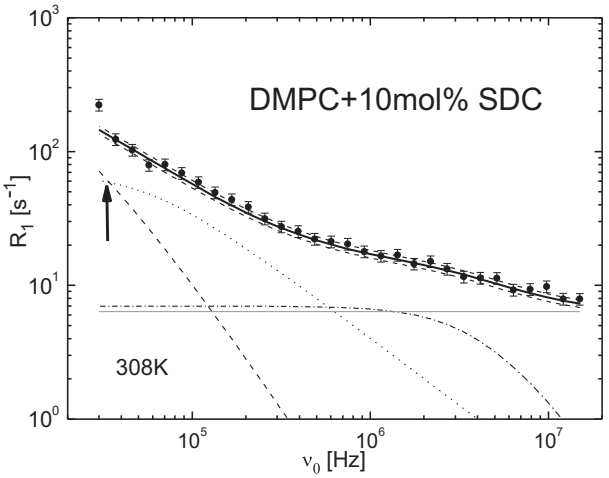

Fig. 4. Relaxation rate dispersion of DMPC + 10 mol% SDC liposomes with average radius of 50 nm, recorded at 308 K. Experimental points are compared with the optimal model curve (black solid line). Model curve error is shown by the two dash lines beside the black solid line. Contributions from each type of motion are included: translational diffusion (dash line), order fluctuations (dot line), molecular rotations (dash-dot line), and fast motions (solid grey line). The relevant parameters are given in Table 1. The arrow indicates the crossing point between order fluctuations and diffusion processes.

deformability and microviscosity are analyzed in similar vesicles (here we are silently assuming that any change in the membrane elasticity will be reflected also in the microviscosity) [27].

The diffusion constant D shows a small increase with SDC concentration (see Table 1). This slight increase is correlated with a decrease in the bending modulus. Also, it is observed that the contribution to the spin-lattice relaxation by diffusion process decreases as the percentage of SDC is increased (compare Figs. 2–5), which is a direct consequence of the fact that the contribution corresponding to order fluctuations becomes dominant at low frequencies. A surprising feature can be observed in these figures: the crossing point between diffusion and order fluctuations contributing relaxation mechanisms is shifting to lower frequencies as the SDC concentration increases. In particular, for 20% of additive, where the R_1 dispersion changes abruptly, this crossing point shifts down by more than an order of magnitude (outside the plot in the figure). In this limit, order fluctuations completely

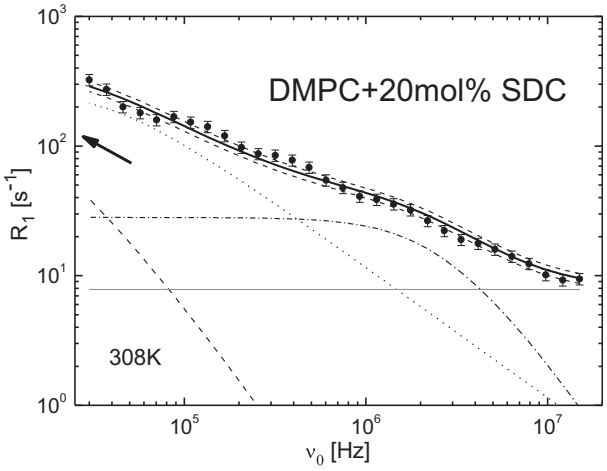

Fig. 5. Relaxation rate dispersion of DMPC + 20 mol% SDC liposomes with average radius of 50 nm, recorded at 308 K. Experimental points are compared with the optimal model curve (black solid line). Model curve error is shown by the two dash lines beside the black solid line. Contributions from each type of motion are included: translational diffusion (dash line), order fluctuations (dot line), molecular rotations (dash-dot line), and fast motions (solid grey line). The relevant parameters are given in Table 1. The arrow indicates the crossing point between order fluctuations and diffusion processes (now shifted to a much lower frequency, see text for explanation).

Table 1
Parameters corresponding to optimal model curves of relaxation dispersions using Eq. (1) for DMPC LUVs with 0, 3, 10 and 20 mol% SDC and average radius of 50 nm, recorded at 308 K (see Figs. 2, 3, 4 and 5). Here N_{data} is number of measured points along the dispersion, N_{manual} is the number of manually discarded data points, $N_{+\,1avg\_curve}$ second elimination of data points (automatic), Δ a number between 0.1 and 0.25, α a number equal or less than Δ/3 and AVG a factor of convergence. See Section "Experimental and methods" for details.

DMPC with different detergent content				
Parameter	Model value			
mol% SDC ± 10%	0	3	10	20
N_{data}	25	30	30	30
N_{manual}	0	2	0	0
$N_{+\,1avg\_curve}$	0	2	1	0
Δ	0.155	0.187	0.182	0.180
α	0.061	0.062	0.090	0.090
κ [J] × 10^{-20}	3.1 ± 0.6	2.5 ± 0.4	2.1 ± 0.2	1.5 ± 0.1
A_{OF} [s^{-2}] × 10^{9}	0.8 ± 0.2	0.6 ± 0.1	0.7 ± 0.1	1.5 ± 0.1
τ_D [s] × 10^{-5}	3.6 ± 0.4	3.3 ± 0.3	2.8 ± 0.3	2.6 ± 0.8
D [m^2/s] × 10^{-12}	8 ± 1	9 ± 1	11 ± 2	12 ± 5
A_D [s^{-2}] × 10^{9}	1.3 ± 0.3	1.0 ± 0.3	0.4 ± 0.1	0.2 ± 0.2
τ_R [s] × 10^{-8}	2.0 ± 0.6	2.6 ± 0.4	2.0 ± 0.3	3.5 ± 0.5
A_R [s^{-2}] × 10^{8}	0.4 ± 0.1	0.5 ± 0.1	0.7 ± 0.1	1.6 ± 0.2
A_{FM} [s^{-1}]	6.8 ± 0.6	7.0 ± 0.5	6.4 ± 0.4	8 ± 1
AVG	0.06	0.08	0.066	0.088

dominate the relaxation dispersion in the low-frequency end of the measured interval. We call this limit for the relaxation regime as the "order fluctuation driven" (OFD), in contrast with the normal regime so far observed in different lipids where diffusion is the dominant contribution at low Larmor frequencies, that is "diffusion driven" (DD).

The rotational correlation time shows-up with a slight increase in response to the SDC content (see Table 1). Finally, A_{OF} and A_R amplitudes show no significant change with the addition of detergent. Additionally, experiments with liposomes of DMPC with 3, 10 and 20 mol % SDC, at 303, 318 and 328 K, were made. Experimental and model dispersion profiles are shown in Section S6 of the Supplementary material, and the corresponding parameters of the optimal model curves are presented in Table 2. It is possible to note a slight tendency in D to increase, while κ and τ_R decrease as temperature increases, at fixed additive concentration. On the other hand, at constant temperature

Table 2
Parameters corresponding to optimal model curves of relaxation dispersions using Eq. (1) for DMPC LUVs with 3, 10 and 20 mol% SDC and average radius of 50 nm, recorded at different temperatures (see Figs. S4, S6–S18).

DMPC at different temperatures and with different detergent content												
Parameter	Model value											
mol% SDC ± 10%	3	3	3	3	10	10	10	20	20	20	20	20
T ± 1 [K]	303	308	318	328	303	308	318	328	303	308	318	328
N_{data}	30	30	30	30	30	30	30	30	30	30	30	30
N_{manual}	2	2	1	3	2	0	1	3	0	0	0	0
$N_{+\,1avg\_curve}$	2	2	1	2	2	1	1	1	1	0	0	2
Δ	0.196	0.187	0.199	0.192	0.180	0.182	0.196	0.202	0.250	0.180	0.180	0.250
α	0.090	0.062	0.070	0.070	0.090	0.090	0.090	0.090	0.090	0.090	0.070	0.100
κ [J] × 10^{-20}	2.9 ± 0.4	2.5 ± 0.0.4	1.5 ± 0.2	1.1 ± 0.3	2.8 ± 0.2	2.1 ± 0.2	1.5 ± 0.2	1.1 ± 0.2	2.4 ± 0.2	1.5 ± 0.1	1.2 ± 0.1	0.9 ± 0.1
A_{OF} [s^{-2}] × 10^{9}	0.4 ± 0.1	0.6 ± 0.1	0.3 ± 0.1	0.2 ± 0.1	1.4 ± 0.1	0.7 ± 0.1	0.2 ± 0.1	0.2 ± 0.1	3.9 ± 0.4	1.5 ± 0.1	0.7 ± 0.1	0.4 ± 0.1
τ_D [s] × 10^{-5}	4.1 ± 0.4	3.3 ± 0.3	2.2 ± 0.3	1.5 ± 0.3	4 ± 1	2.8 ± 0.3	2.0 ± 0.2	1.4 ± 0.3	3.8 ± 0.7	2.6 ± 0.8	1.9 ± 0.8	1.0 ± 0.7
D [m^2/s] × 10^{-12}	7 ± 1	9 ± 1	14 ± 3	22 ± 6	8 ± 3	11 ± 2	16 ± 2	24 ± 6	8 ± 2	12 ± 5	17 ± 9	36 ± 30
A_D [s^{-2}] × 10^{9}	1.3 ± 0.2	1.0 ± 0.3	0.6 ± 0.1	0.5 ± 0.2	0.3 ± 0.1	0.4 ± 0.1	0.7 ± 0.1	0.5 ± 0.2	0.3 ± 0.1	0.2 ± 0.2	0.20 ± 0.08	0.10 ± 0.07
τ_R [s] × 10^{-8}	3.1 ± 0.5	2.6 ± 0.4	1.5 ± 1.0	0.5 ± 0.4	2.4 ± 0.2	2.0 ± 0.3	1.5 ± 0.2	0.8 ± 0.2	4.3 ± 0.4	3.5 ± 0.5	2.9 ± 0.8	1.8 ± 0.6
A_R [s^{-2}] × 10^{8}	0.8 ± 0.1	0.5 ± 0.1	0.2 ± 0.1	0.3 ± 0.1	1.0 ± 0.1	0.7 ± 0.1	0.7 ± 0.1	0.3 ± 0.1	2.1 ± 0.2	1.6 ± 0.2	0.9 ± 0.2	0.7 ± 0.1
A_{FM} [s^{-1}]	7.8 ± 0.3	7.0 ± 0.5	5.3 ± 0.4	3.5 ± 0.4	7.7 ± 0.5	6.4 ± 0.4	4.5 ± 0.5	3.8 ± 0.4	9.1 ± 0.9	8 ± 1	5.6 ± 0.8	4.7 ± 0.9
AVG	0.101	0.080	0.068	0.085	0.093	0.066	0.074	0.089	0.086	0.088	0.055	0.083

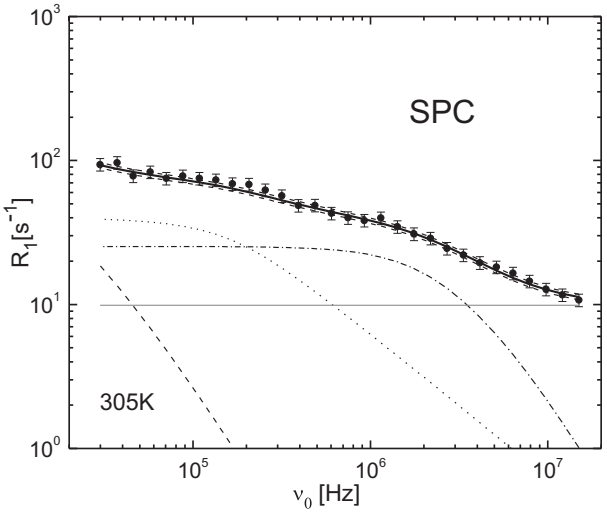

Fig. 6. Relaxation rate dispersion of SPC liposomes with average radius of 50 nm, recorded at 305 K. Experimental points are compared with the optimal model curve (black solid line). Model curve error is shown by the two dash lines beside the black solid line. Contributions from each type of motion are included: translational diffusion (dash line), order fluctuations (dot line), molecular rotations (dash-dot line), and fast motions (solid grey line). The relevant parameters are given in Table 3.

(303, 318 or 328 K), same tendencies are observed in terms of SDC content.

2.2.2. Liposomes of SPC + SDC

Experimental relaxation rate dispersion curves and their optimal model curves for SPC liposomes, with 0 and 20 mol% SDC, at 305 K are shown in Figs. 6 and 7, respectively. Corresponding parameters are presented in Table 3. A very surprising feature is that in this case, even in the absence of additive, the low-frequency relaxation dispersion follows an OFD regime, in similitude to DMPC + 20 mol% SDC profiles (compare Fig. 5 with Figs. 6 and 7). There is a very good agreement (within experimental errors) between the model curves and data for both additivated and non-additivated liposomes (see Figs. 6 and 7). The numerical values of all parameters are within the expected range according to literature [16–26].

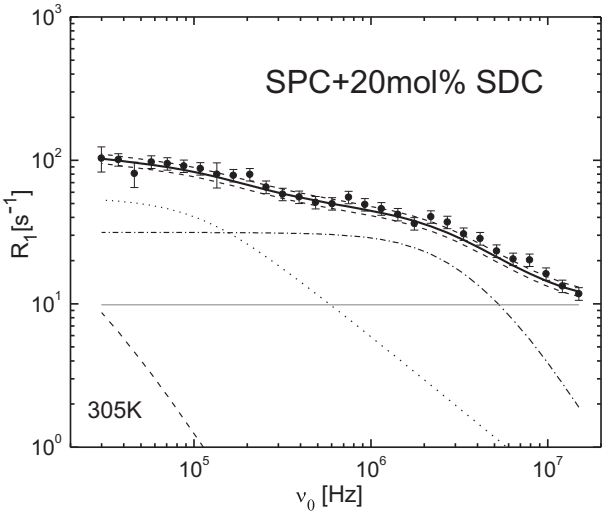

Fig. 7. Relaxation rate dispersion of SPC + 20 mol% liposomes with average radius of 50 nm, recorded at 305 K. Experimental points are compared with the optimal model curve (black solid line). Model curve error is shown by the two dash lines beside the black solid line. Contributions from each type of motion are included: translational diffusion (dash line), order fluctuations (dot line), molecular rotations (dash-dot line), and fast motions (solid grey line). The relevant parameters are given in Table 3.

The bending elastic modulus κ shows a slight tendency to decrease as the percentage of detergent increases (see Table 3). The fact that κ do not show a large variation is consistent with other studies reporting minor changes in the membrane microviscosity [27].

The rotational correlation time τ_R slightly decreases in response to the additive content (see Table 3), while A_{OF} and A_R amplitudes show no significant change with additive concentration. In contrast, the diffusion constant D shows a small increase with detergent content (see Table 3). An OFD regime is evidenced independently of the SDC concentration, and the diffusion contribution to the spin-lattice relaxation turns irrelevant as the percentage of detergent is increased (compare Figs. 6 and 7). This effect is reflected in anomalous variations of A_D and big errors associated to D and τ_D. This essentially means that lipid diffusion is not an effective relaxation mechanism anymore, and experimental curves might be analyzed in terms of a simplified model excluding this contribution. Therefore, a simplified version of the model was used to describe the measured dispersions, as shown in Figs. 8 and 9, by only considering order fluctuations, molecular rotations, and intramolecular fast motions. No significant variations in the parameters, within experimental errors, are observable in comparison with the full model Eq. (1). Moreover, κ and τ_R can be determined with higher accuracy using the simplified model (see errors in Table 3).

Additionally, experiments using SPC liposomes with (20 mol%) and without SDC were made at 313 K. Experimental data and model curve are displayed in Figs. S15 and S16 while the corresponding parameters of the optimal model curves are depicted in Table 3.

It is possible to note a slight tendency in D to increase and in κ and τ_R to decrease as temperature increases, at fixed detergent content. On the other hand, at 313 K, same tendencies are observed in all parameters as described for liposomes at 305 K, as detergent content increases. The analysis without considering diffusion process for profiles at 313 K was also carried out and it is shown in Figs. S17 and S18. Corresponding parameters using simplified model are displayed in Table 3. Again, no significant changes are observed in the parameters, within experimental errors, when compared to those obtained using the complete model, and the parameters κ and τ_R can be calculated with higher accuracy when the simplified model is used (see errors in Table 3).

3. Discussion

The lipid molecular dynamics of DMPC and SPC liposomes additivated with SDC were successfully described using the model of Eq. (1). All physical parameters showed the expected tendency as a function of temperature (for increasing temperature, a decrease of the bending modulus and correlation times is expected, while minor differences should be expected in the spectral density amplitudes). A simplified version of the model was proposed to describe SPC liposomes dispersions due to a remarkable OFD regime, turning the diffusion contribution to spin-relaxation irrelevant compared to the order fluctuation process. This tendency was also observed for DMPC additivated liposomes at the higher concentration. A direct explanation for this behavior might be that shape fluctuations enhances as detergent content increases, thus favoring order fluctuations over diffusion, as reflected in the proton spin-relaxation. A word of caution should be mentioned at this point: this result does not mean that lipids do not diffuse in the membrane, but thermal order fluctuations become much more effective in relaxing the proton Zeeman energy than diffusion.

An enhanced elasticity should be reflected in a decrease of κ, as observed. However, we see that in general changes in κ due to additive concentration are less relevant to those originated in a change of temperature. For instance, κ becomes independent on the SDC concentration as the DMPC + SDC mixture approaches the superelastic limit $\kappa \sim K_BT$ (see Fig. 10 and Table 2). Moreover, we can see that for 318 K and 328 K changes in κ with the SDC content are negligible. According to the basic statements of the continuum theory (Section S1), this

Table 3
Parameters corresponding to optimal model curves of relaxation dispersions using Eq. (1) with and without diffusion process for SPC LUVs with (20 mol%) and without SDC, and average radius R_0 = 50 nm, recorded at different temperatures (see Figs. 5-8 and S15–S18).

SPC at different temperatures and with different detergent content								
Parameter	Model value							
	Model with diffusion				Model without diffusion			
mol% SDC ± 10%	0	0	20	20	0	0	20	20
T ± 1 [K]	305	313	305	313	305	313	305	313
N_{data}	30	30	30	30	30	30	30	30
N_{manual}	0	0	0	0	0	0	0	0
N_{+1avg_curve}	0	0	1	0	0	0	0	0
Δ	0.15	0.15	0.20	0.20	0.15	0.18	0.18	0.20
α	0.05	0.05	0.09	0.08	0.05	0.06	0.07	0.08
κ [J] × 10^{-20}	6.3 ± 0.8	5.1 ± 0.5	4.3 ± 0.5	3.9 ± 0.3	5.8 ± 0.2	4.7 ± 0.2	4.0 ± 0.3	3.7 ± 0.2
A_{OF} [s^{-2}] × 10^9	3.5 ± 0.7	2.7 ± 0.5	2.2 ± 0.5	2.5 ± 0.2	3.8 ± 0.2	3.3 ± 0.2	2.0 ± 0.3	2.5 ± 0.2
τ_D [s] × 10^{-5}	3.6 ± 1.5	3.2 ± 1.9	2.3 ± 1.7	1.8 ± 1.4	–	–	–	–
D [m^2/s] × 10^{-12}	8 ± 5	9 ± 8	14 ± 13	19 ± 18	–	–	–	–
A_D [s^{-2}] × 10^8	1.0 ± 0.6	1.0 ± 0.6	0.3 ± 0.4	0.4 ± 0.4	–	–	–	–
τ_R [s] × 10^{-8}	3.2 ± 0.6	2.1 ± 0.4	2.6 ± 0.5	1.8 ± 0.3	3.1 ± 0.3	1.9 ± 0.3	2.4 ± 0.3	1.8 ± 0.3
A_R [s^{-2}] × 10^8	1.6 ± 0.3	1.7 ± 0.2	2.4 ± 0.3	2.0 ± 0.2	1.7 ± 0.1	1.5 ± 0.2	2.8 ± 0.3	2.3 ± 0.3
A_{FM} [s^{-1}]	9.9 ± 1.1	7.3 ± 1.2	9.8 ± 1.1	7.2 ± 0.9	9.3 ± 1.0	7.2 ± 0.8	9.4 ± 1.2	6.5 ± 0.6
AVG	0.044	0.045	0.084	0.08	0.043	0.057	0.064	0.077

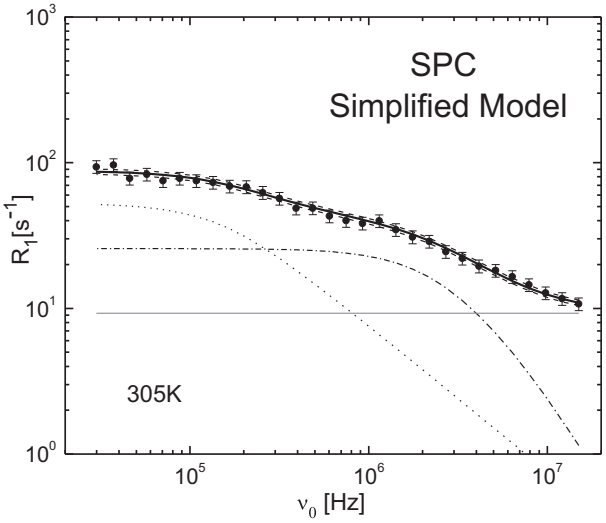

Fig. 8. Relaxation rate dispersion of SPC liposomes with average radius of 50 nm, recorded at 305 K. Experimental points are compared with the optimal model curve obtained from the simplified model without diffusion process (black solid line). Model curve error is shown by the two dash lines beside the black solid line. Contributions from each type of motion are included: order fluctuations (dot line), molecular rotations (dash-dot line), and fast motions (solid grey line). The relevant parameters are given in Table 3.

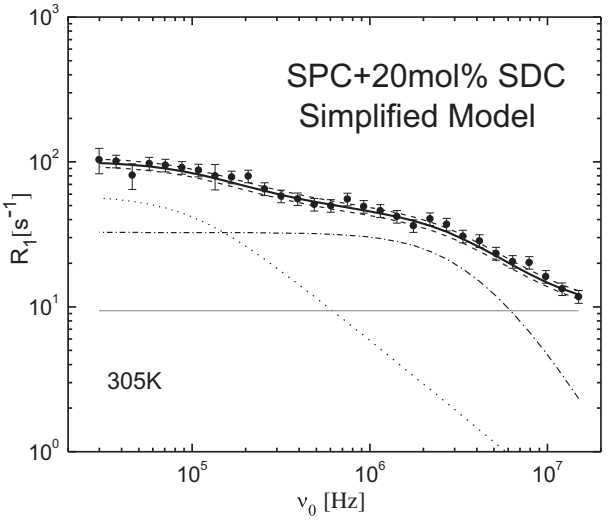

Fig. 9. Relaxation rate dispersion of SPC + 20 mol% SDC liposomes with average radius of 50 nm, recorded at 305 K. Experimental points are compared with the optimal model curve obtained from the simplified model without diffusion process (black solid line). Model curve error is shown by the two dash lines beside the black solid line. Contributions from each type of motion are included: order fluctuations (dot line), molecular rotations (dash-dot line), and fast motions (solid grey line). The relevant parameters are given in Table 3.

behavior may be interpreted as a deficient coupling of the additive and the local curvature. Consequently, the curvature instability does not manifest at the explored SDC concentrations and temperatures: hydrodynamic mode amplitudes are mainly governed by K_BT while $\zeta^2/a \ll K_BT$ (for a large quantity of modes, see Eq. (S18)). However, we may consider the abrupt switch of the nuclear relaxation to an OFD regime as an early manifestation of such kind of instability. That is, the proton magnetic relaxation is sensitive to pre-critical effects that are still not reflected in the mesoscopic elastic behavior of the membrane.

In spite of the fact that SDC and SPC have been established as standard components to prepare elastic liposomes in the literature, it was not possible to observe large variations in κ as detergent content increases up to 20 mol%. However, the observed changes as a function of concentration are higher than those observed for the DMPC case, at both temperatures (see Tables), suggesting a more efficient ζ in the case of DMPC + SDC mixture. Other authors have reported great variations (around 80%) in κ for additivated SPC liposomes using a nonionic detergent (around 20 mol%) [25]. In contrast, SDC as used here is ionic. This disagreement might be due to electrostatic effects [28]. In fact, different membrane properties (permeability, elasticity, fluidity, etc.) of phospholipid-detergent mixtures may depend on the ionic character of the additive [29,30]. The electrostatic contribution to the elastic properties of a mixture has been scarcely considered in the literature [28]. The topic deserves a more careful examination.

Obtained values of κ for unadditivated DMPC can be compared to the values obtained by other authors. In this work, the values obtained at 303 K and 310 K do not change within errors, being about 3×10^{-20} J. The same behavior was observed using phase contrast video microscopy, but a value four times larger have been reported [21]. Differences may be attributed to both the sample preparation and the used techniques. A more general discussion on this point can be found in the literature [1,3,28,31–34]. Particular assumptions in the theoretical models used to interpret data obtained with different

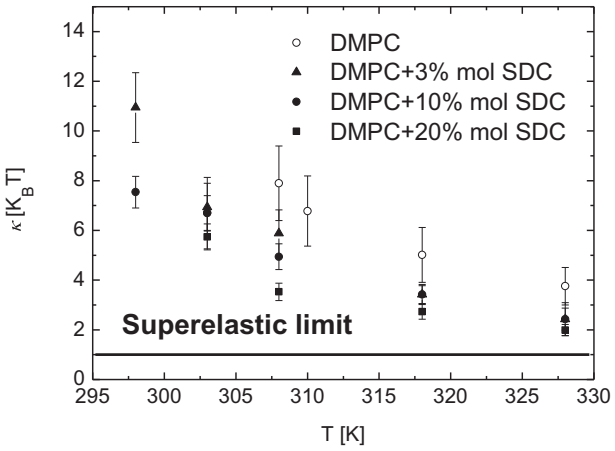

Fig. 10. Comparison of κ as a function of temperature for different concentrations of SDC in DMPC. The system approaches the superelastic limit as temperature increases. The graph also includes data for 3% and 10% measured at 298 K, not reported in Table 2.

experimental techniques, as different needs for the sample preparation, may affect the obtained value. Even when NMR has the benefit of being quite non-invasive, a deeper understanding of such differences must be carefully considered in future work.

A word of caution should be expressed about differences between proton and ^{2}H and ^{13}C NMR relaxation dispersions in unilamellar vesicles. While our model predicts a flatter dispersion over 10 MHz corresponding to local internal fast motions of the lipids for protons, ^{2}H and ^{13}C show a well-defined dispersion that is observable up to 100 MHz for ^{2}H and 200 MHz for ^{13}C [35]. In the lipids, protons are mainly located in the aliphatic chains, and associated to CH2 and CH3 groups. At high frequencies fast local segmental fluctuations of the protons belonging to these groups start to be efficient for the proton relaxation. Protons undergo into rotations, librations and vibrations with a lower restriction in these groups. At low Larmor frequencies, these fast fluctuations averages the dipolar interaction into a residual "static" component that is modulated by highly correlated collective motions and/or diffusion. In contrast, direct C—C interactions are negligible since ^{13}C has a much lower natural abundance. Inter-chain C—C interactions are supposedly very scarce for the same reason and the high mobility of the chains. However, C—H interactions, due to the topology of the chain and the higher mobility restriction of the carbon, still has an effective residual dipolar coupling at higher frequencies that is modulated by collective fluctuations. This would explain why carbon 13 is sensitive to a dispersion that extends up to the high frequency-end of the measured data presented by NB, while we do not see such extension in protons. Concerning ^{2}H, the quadrupolar moment of the deuterons interacts with the surviving electric field gradient (EFG) of the bond. Even when motional narrowing can be very effective in reducing the quadrupolar splitting of the spectrum, clearly relaxation is due to the fluctuating interaction of the quadrupolar moment and the EFG. Similarly to the ^{13}C case, here the dynamical average leaves a non-zero averaged EFG, and the interaction becomes modulated by those fluctuations surviving the dynamic average, due to their collective nature (strongly correlated versus not-correlated motions). Since the bond is directed towards a carbon, the fluctuation has the same power spectrum of the case of the carbon-proton pair. Consequently, the spectral density is also the same (as the authors claim in their manuscript).

It is also worth to mention ^{31}P relaxation experiments using a sample-shuttling field-cycling approach [36]. Using a free-model approach to explain the measured dispersions in diverse vesicles and micelles formulations, the authors conclude that collective motions are unlikely to couple to relative phosphorus-proton motion with the required amplitude, and that they are not needed to explain the observed results [37]. According to this result, 31P relaxation is not a good choice to assess the elastic properties of the membrane.

4. Conclusions

We have shown the potentiality of the FFC-NMR technique for the study and characterization of elastic liposomes. The technique allows addressing details of the molecular dynamics of the lipids over a wide timescale, with the simultaneous possibility of measuring the elastic bending modulus κ. The specific advantage of the experiment is the ability to provide information on membrane rigidity and lipid lateral mobility from the same measured dispersion, in a non-invasive/non-destructive way.

We report a new relaxation dispersion regime that has never been observed before in liposomes, as a consequence of adding an ionic detergent to DMPC, and even without additive in SPC. Variations in κ are moderate in response to the additive concentration up to 20 mol% for the both studied cases. However, we observe dramatic changes in the way diffusion and order fluctuations affect the proton spin-lattice relaxation as SDC concentration is increased. In particular, the concentration dependence of κ close to the superelastic limit disappears for the DMPC + SDC mixture. Changes in κ in terms of SDC concentration are higher for SPC compared to DMPC. In contrast, changes in κ as a function of temperature are more relevant in both cases.

A previously validated model that explains the observed relaxation dispersion based on the molecular dynamics of lipids has been successfully used in this study. This model allows estimating the bending elastic modulus κ of liposome membranes non-invasively. A simplified version of this model was proposed in cases where order fluctuations became the dominant relaxation mechanism al low Larmor frequencies (we call it OFD regime). This feature turned to be more evident for the SPC + SDC mixture than for the DMPC + SDC case. No significant variations were observed in physical parameters, within experimental errors, as compared to those obtained using the complete model, and they can be calculated with higher accuracy when the simplified model is used.

5. Experimental and methods

5.1. Automatic analysis of relaxation rate dispersions

We introduce an automatic method to interpret the experimental relaxation rate dispersions R_1 of protons in unilamellar liposomes using the model given by the Eq. (1). That is, a method used to obtain the optimal model curve that better describes the experimental data. This is important to standardize the systematic analysis of the measured dispersion curves, while saving a huge amount of time (as previously employed in the manual analysis).

Three relevant physical parameters (κ, τ_D, τ_R) [12], three amplitudes (A_{OF}, A_D, A_R) and one constant (A_{FM}) emerge from the model. Therefore, it could be said that it is necessary to determine the values of seven parameters to calculate the optimal curve. In previous works the procedure to get that optimal curve was based on fixing the relevant physical parameters within their most probable intervals using literature values [12–14], and then on minimizing the sum of the squared differences between the simulated curve and the experimental data manually. This approach worked very well although it was not very efficient because of being a time consuming procedure. Therefore, in order to implement an automatic methodology to treat data from different samples with a single criterion, the following systematic approach was adopted:

1) Manual elimination of experimental points N_{manual} that are clearly outside the tendency of the experimental curve, that is, those which are distinguishable by being out of the statistical dispersion of points along the measured relaxation rate dispersion. Remaining points are R_{1i}^{exp}.

2) Random assignment of values for all the aforementioned parameters within their most probable intervals, considering the following initial restriction:

$$\frac{|R_{1i}^{exp} - R_{1i}^{mod}|}{R_{1i}^{exp}} \leq \Delta,\ i = 1,\ ..., N_{data} - N_{manual} \quad (4)$$

where $R_{1i}{}^{mod}$ represent the model R_1 values at the frequencies ν_{0i}, respectively. Δ is a number (usually between 0.1 and 0.25) calculated for each experimental curve and it was defined as follows:

$$\Delta = 3*\text{maxvalue}\left(\frac{|(R_{li-1}^{exp} + R_{li+1}^{exp}/2 - R_{li}^{exp})|}{R_{li-1}^{exp} + R_{li+1}^{exp}/2}\right),\ i = 2,\ ...,\ (N_{data} - N_{manual}) - 1 \quad (5)$$

3) Calculation of the fitting curve using the following convergence and optimization criterion:

$$AVG = {}^{1}\!/_{(N_{data} - N_{manual})} \sum_{i} \frac{|R_{1i}^{exp} - R_{1i}^{mod}|}{R_{1i}^{exp}} \leq a,\quad i = 1,\ ...,\ N_{data} - N_{manual} \quad (6)$$

where α is a number that is less or equal to Δ/3 (usually between 0.04 and 0.1).

4) Second elimination of experimental points $N_{+\,1avg\_curve}$ using the next condition:

$$|(R_{1i}^{exp} \pm \sigma_i^{exp}) - R_{1i}^{mod}| \leq AVG \times R_{1i}^{mod} = \sigma_{fitting}^{i},\quad i = 1,\ ...,\ N_{data} \quad (7)$$

where $\sigma_i{}^{exp}$ is the experimental error corresponding to $R_{1i}{}^{exp}$ and $\sigma_{fitting}^{i}$ represents the error corresponding to $R_{1i}{}^{mod}$.

5) Calculation of the new fitting curve using $(N_{data} - N_{+\,1avg\_curve})$ points under the conditions given by the Eqs. (4) and (6).
6) Steps 4 and 5 are repeated if necessary.

The validation and application of the method can be found in the Supplementary material.

5.2. Liposome preparation

Large unilamellar vesicle (LUV) suspensions of 1,2-dimyristoyl-*sn*-glycero-3-phosphocholine (DMPC) or soybean phosphatidylcholine (SPC), were prepared using the same methodology as in previous works [3,12–14]. Some of them were made with cholesterol (3 mol%) or sodium deoxycholate (SDC) (3, 10, and 20 mol%), where the detergent SDC was used as edge activator for deformable liposomes. A lipid film was prepared by dissolving lipid + cholesterol in 2 ml $CHCl_3$, or lipid + detergent mixtures in $CHCl_3$ + methanol. Once mixed, the solvent was removed to yield the lipid film under a dry nitrogen flow. Lipid film was then thoroughly dried by placing the flask on a vacuum pump for 3 h. Following hydration by adding 1.5 ml D_20, the suspension was exposed to 5 freeze-thaw cycles using liquid nitrogen and warm water (313 K). After completing the thermal treatment, the suspension was passed through an Avanti Polar Lipids (Alabaster - USA) mini extruder containing polycarbonate membranes with a pore size of 0.1 μm. The extrusion process was carried out above the main phase transition temperature T_m. The average sizes of the obtained unilamellar liposomes were determined using a Nicomp 380 High Performance Particle Sizer (HPPS). Experiments were performed on liposome suspensions of DMPC with 0 and 3 mol% cholesterol, DMPC with 0, 3, 10 and 20 mol% SDC, and SPC with 0 and 20 mol% SDC, all of them in the liquid crystalline phase. The average hydrodynamic radium was 50 nm in all cases, and the employed temperatures were between 303 and 328 K (± 1 K).

5.3. Relaxation rate dispersion experiments

^{1}H relaxation rate dispersions were measured using a Spinmaster FC2000/C/D Relaxometer (Stelar; Mede, Italy) for liposome samples of 1 ml. In all cases a polarization and acquisition magnetic fields of 0.375 T (equivalent to 15 MHz for ^{1}H) were used. Profiles were measured within the frequency range from 30 kHz to 15 MHz (relaxation magnetic field values). The relaxation rates, R_1, were determined from the magnetization recovery curves. Measured R_1 values were not sensitive to the time window over which the NMR signal was acquired (after a 90° pulse). The spin relaxation process for all samples was found to be mono-exponential, within errors, at all frequencies. The sample temperature was controlled within ± 1 K using the Spinmaster Variable Temperature Controller (VTC). The VTC temperature measurement was previously calibrated using a Cu–Al thermocouple glued into a 10 mm NMR tube connected to a CHY 503 electronic thermometer.

It is worth mentioning that in our samples there are protons in lipids, in the detergent molecules (less than 12% of the total protons population in the worst case) and eventually in HDO molecules formed during the sample preparation. Like in the case of cholesterol mixtures, SDC molecules follow lipids dynamics in first approximation when they are intercalated into the lipid bilayer [14]. The contribution to the relaxation rate due to free molecules of HDO, as they belong to the bulk water, is non-dispersive within the measured frequency range (and therefore absorbed into A_F). Associated HDO molecules that may exchange with the bulk, although an efficient relaxation mechanism, may be considered as a second-order correction of the employed model (as the concentration is very low). For the same reason, HDO molecules having a long residence time on the lipid chains, can also be neglected in a first approximation. At higher concentrations, the coupling of bound HDO with lipid protons may offer an additional relaxation channel. On the other hand, possible effects on the relaxation dispersion due to detergent molecules that are not bound to the lipid bilayer were analyzed, both in free-state (no aggregation) and after micellar aggregation. Experiments showed that they are not dispersive in the considered frequency range.

The automatic protocol for curve fitting previously described showed to work properly, and obtained results are consistent with the literature. The methodology resembles a least squares fitting procedure, but in this case absolute differences between the model and experimental values are minimized instead. This practice reduces the computing time, while the final result is not critically dependent on this choice. The model curve obtained with this methodology is actually a sub-optimal curve considering that its calculation depends on the random parameters taken in the first steps of the method. Nevertheless, this simple approach was used since it is directly derived from the manual procedure that has been used in previous works [12–14]. The method may be improved by using genetic algorithms or more sophisticated mathematical tools, but they would also converge to sub-optimal solutions, without major changes in the physical significance of the result. In any case, the described approach should be refined in the future, incorporating an efficient algorithm for the automatic elimination of experimental data points that are out of tolerance.

Acknowledgements

This work was financed by Fondo para la Investigación Científica y Tecnológica (FONCYT) under contract PICT-2013-1380, Ministerio de Ciencia y Tecnología de la Provincia de Córdoba and Secyt-UNC (05/B479). The authors acknowledge Dr. Guillermo Montich and CIQUIBIC for the access to their infrastructure for sample preparation.

Appendix A. Supplementary data

Supplementary data to this article can be found online at http://dx.doi.org/10.1016/j.bpc.2017.06.007.

References

[1] R. Dimova, Recent developments in the field of bending rigidity measurements on membranes, Adv. Colloid Interf. Sci. 208 (2014) 225–234.
[2] C. Monzel, K. Sengupta, Measuring shape fluctuations in biological membranes, J. Phys. D. Appl. Phys. 49 (2016) 243002–243023.
[3] G.A. Domingez, J. Perlo, C.C. Fraenza, E. Anoardo, Measurement of the bending elastic modulus in unilamellar vesicles membranes by fast field cycling NMR relaxometry, Chem. Phys. Lipids 201 (2016) 21–27.
[4] G. Cevc, Lipid vesicles and other colloids as drug carriers on the skin, Adv. Drug Deliv. Rev. 56 (2004) 675–711.
[5] S. Duangjit, Y. Obata, H. Sano, Y. Onuki, P. Opanasopit, T. Ngawhirunpat, T. Miyoshi, S. Kato, K. Takayama, Comparative study of novel ultradeformable liposomes: menthosomes, transfersomes and liposomes for enhancing skin permeation of meloxicam, Biol. Pharm. Bull. 37 (2014) 239–247.
[6] J.E. Shaw, S.K. Chandrasekaran, M.W. Greaves, S. Shuster (Eds.), Pharmacology of the Skin II, Springer-Verlag, Berlin, 1989(Ch. 13).
[7] G. Cevc, A.G. Schätzlein, H. Richardsen, U. Vierl, Overcoming semipermeable barriers, such as the skin, with ultradeformable mixed lipid vesicles, transfersomes, liposomes, or mixed lipid micelles, Langmuir 19 (2003) 10753–10763.
[8] G. Cevc, D. Gebauer, Hydration-driven transport of deformable lipid vesicles through fine pores and the skin barrier, Biophys. J. 84 (2003) 1010–1024.
[9] M. Boncheva, J. De Sterke, P.J. Caspers, G.J. Puppels, Depth profiling of stratum corneum hydration in vivo: a comparison between conductance and confocal Raman spectroscopic measurements, Exp. Dermatol. 18 (2009) 870–876.
[10] O.G. Mouritsen, L. Bagatoli, Life as a Matter of Fat: Lipids in a Membrane Biophysics Perspective, Springer, Heidelberg, 2016.
[11] R. Kimmich, E. Anoardo, Field-cycling NMR relaxometry, Prog. Nucl. Magn. Reson. Spectrosc. 44 (2004) 257–320.
[12] C.J. Meledandri, J. Perlo, E. Farrher, D.F. Brougham, E. Anoardo, Interpretation of molecular dynamics on different time scales in unilamellar vesicles using field-cycling NMR relaxometry, J. Phys. Chem. B 113 (2009) 15532–15540.
[13] J. Perlo, C.J. Meledandri, E. Anoardo, D.F. Brougham, Temperature and size- dependence of membrane molecular dynamics in unilamellar vesicles by fast field-cycling NMR relaxometry, J. Phys. Chem. B 115 (2011) 3444–3451.
[14] C.C. Fraenza, C.J. Meledandri, E. Anoardo, D.F. Brougham, The effect of cholesterol on membrane dynamics on different timescales in lipid bilayers from fast field-cycling NMR relaxometry studies of unilamellar vesicles, ChemPhysChem 15 (2014) 425–435.
[15] M. Vilfan, G. Althoff, I. Vilfan, G. Kothe, Nuclear-spin relaxation induced by shape fluctuations in membrane vesicles, Phys. Rev. E 64 (2001) 022902.
[16] E. Wu, K. Jacobson, D. Papahadjopoulos, Lateral diffusion in phospholipid multibilayers measured by fluorescence recovery after photobleaching, Biochemistry 16 (1977) 3936–3941.
[17] W.L. Vaz, M. Criado, V.M. Madeira, G. Schoellmann, T.M. Jovin, Size dependence of the translational diffusion of large integral membrane proteins in liquid-crystalline phase lipid bilayers. A study using fluorescence recovery after photobleaching, Biochemistry 21 (1982) 5608–5612.
[18] L.K. Tamm, H.M. McConnell, Supported phospholipid bilayers, Biophys. J. 47 (1985) 105–113.
[19] H.P. Duwe, E. Sackmann, Bending elasticity and thermal excitations of lipid bilayer vesicles: modulation by solutes, Phys. Stat. Mech. Appl. 163 (1990) 410–428.
[20] P.F. Almeida, W.L. Vaz, T.E. Thompson, Lateral diffusion in the liquid phases of dimyristoylphosphatidylcholine/cholesterol lipid bilayers: a free volume analysis, Biochemistry 31 (1992) 6739–6747.
[21] P. Meleard, C. Gerbeaud, T. Pott, L. Fernandez-Puente, I. Bivas, M.D. Mitov, J. Dufourcq, P. Bothorel, Bending elasticities of model membranes: Influences of temperature and sterol content, Biophys. J. 72 (1997) 2616–2629.
[22] A. Filippov, G. Orädd, G. Lindblom, The effect of cholesterol on the lateral diffusion of phospholipids in oriented bilayers, Biophys. J. 84 (2003) 3079–3086.
[23] A. Filippov, G. Orädd, G. Lindblom, Influence of cholesterol and water content on phospholipid lateral diffusion in bilayers, Langmuir 19 (2003) 6397–6400.
[24] P.F. Almeida, W.L. Vaz, T.E. Thompson, Lipid diffusion, free area, and molecular dynamics simulations, Biophys. J. 88 (2005) 4434–4438.
[25] C. Wachter, U. Vierl, G. Cevc, Adaptability and elasticity of the mixed lipid bilayer vesicles containing non-ionic surfactant designed for targeted drug delivery across the skin, J. Drug Target. 16 (2008) 611–625.
[26] J. Pan, T.T. Mills, S. Tristram-Nagle, J.F. Nagle, Cholesterol perturbs lipid bilayers nonuniversally, Phys. Rev. Lett. 100 (2008) 198103–198107.
[27] A. Gillet, A. Grammenos, P. Compère, B. Evrard, G. Piel, Development of a new topical system: drug-in-cyclodextrin-in-deformable liposome, Int. J. Pharm. 380 (2009) 174–180.
[28] A.C. Rowat, P.L. Hansen, J.H. Ipsen, Experimental evidence of the electrostatic contribution to membrane bending rigidity, Europhys. Lett. 67 (2004) 144–149.
[29] D. Lichtenberg, R.J. Robson, E.A. Dennis, Solubilization of phospholipids by detergents structural and kinetic aspects, Biochim. Biophys. Acta 737 (1983) 285–304.
[30] G.M. Zaafarany, G.A.S. Awad, S.M. Holayel, N.D. Mortada, Role of edge activators and surface charge in developing ultradeformable vesicles with enhanced skin delivery, Int. J. Pharm. 397 (2010) 164–172.
[31] A.C. Rowat, J. Brask, T. Sparrman, K.J. Jensen, G. Lindblom, J.H. Ipsen, Farnesylated peptides in model membranes: a biophysical investigation, Eur. Biophys. 33 (2004) 300–309.
[32] J.F. Nagle, Introductory lecture: basic quantities in model biomembranes, Faraday Discuss. 161 (2013) 11–29.
[33] H. Bouvaris, L. Duelund, J.H. Ipsen, Buffers affect the bending rigidity of model lipid membranes, Langmuir 30 (2014) 13–16.
[34] J.F. Nagle, M.S. Jablin, S. Tristam-Nagle, K. Akabori, What are the true values of the bending modulus of simple lipid bilayers? Chem. Phys. Lipids 185 (2015) 3–10.
[35] A.A. Nevzorov, M.F. Brown, Dynamics of lipid bilayers from comparative analysis of ^{2}H and ^{13}C nuclear magnetic resonance relaxation data as a function of frequency and temperature, J. Chem. Phys. 107 (1997) 10288–10310.
[36] A.G. Redfield, High resolution NMR field-cycling device for full-range relaxation and structural studies of biopolymers on a shared commercial instrument, J. Biomol. NMR 52 (2012) 159–177.
[37] M.F. Roberts, A.G. Redfield, High resolution ^{31}P field-cycling NMR as a probe of phospholipid dynamics, J. Am. Chem. Soc. 126 (2004) 13765–13777.